

## Conclusion

This work demonstrates that the segmental ordering induced in strained networks depends largely on the conditions of the network synthesis. For instance, a variation of only 10% in the polymer fraction during the cross-linking process has a noticeable effect on the induced orientational anisotropy. Quantitatively, we find that the degree of order  $\langle P_2 \rangle$  goes like the degree of equilibrium swelling  $\Phi_e$ . Since this phenomenological scaling law is the same as that obtained by varying the cross-linking density, the present study strongly supports our previous conclusion:<sup>8</sup>  $\Phi_e$  is the thermodynamical variable well adapted to precisely define the real topological structure of the network, with respect to the orientational chain ordering.

In contrast, neutron scattering measurements show that the physical constraints have no noticeable effect on the mesh size. Therefore, a better understanding of the difference between the response obtained from the NMR and the SANS experiments could provide useful information. Particularly, it is important to determine whether the concept of sliplinks is compatible with trapped entanglements acting on the molecular ordering only but without changing the overall dimensions of the distorted chains.

Finally, concerning the experimental approach, let us notice that the present work emphasizes the reliability and the sensitivity of the solvent-probe method for testing orientational order in rubbers; indeed it leads to the same result as those obtained from direct investigation of the polymer chain. Thus, this probe method appears to be a very attractive tool since it allows us to obviate the perturbations of conventional probe techniques (electron spin resonance, fluorescence) while providing reliable information on local chain behavior.

**Acknowledgment.** It is a pleasure to acknowledge J. F. Joanny (University C. Bernard, Lyon), J. Bastide and A. Lapp (C.R.M., Strasbourg) and F. Boué (L.L.B., Saclay) for their stimulating discussions through the course of this work.

## References and Notes

- (1) Candau, S.; Peters, A. *Polymer* 1981, 22, 1504.
- (2) Beltzung, M.; Picot, C.; Herz, J. *Macromolecules* 1984, 17, 663.
- (3) Vasiliev, V. G.; Rogovina, L. Z.; Slonimsky, G. L. *Polymer* 1985, 26, 1667.
- (4) Herz, J.; Munch, J. P.; Candau, S. *J. Macromol. Sci., Phys.* 1980, B18, 267.
- (5) Monnerie, L. *Faraday Symp. Chem. Soc.* 1983, 18, paper 5.
- (6) Cohen-Addad, J. P.; Domard, M.; Herz, J. *J. Chem. Phys.* 1982, 76, 2744.
- (7) Deloche, B.; Samulski, E. T. *Macromolecules* 1981, 14, 575.
- (8) Dubault, A.; Deloche, B.; Herz, J. *Polymer* 1984, 25, 1405.
- (9) Cohen-Addad, J. P.; Domard, M.; Lorentz, G.; Herz, J. *J. Phys. (Les Ulis, Fr.)* 1984, 45, 575.
- (10) Beltzung, M. Thesis, Strasbourg, 1982.
- (11) Beltzung, M.; Picot, C.; Rempp, P.; Herz, J. *Macromolecules* 1982, 15, 1594.
- (12) Charvolin, J.; Deloche, B. *The Molecular Physics of Liquid Crystals*; Luckhurst, G. R., Gray, G. W., Eds.; Academic: London, 1979; Chapter 15.
- (13) Samulski, E. T. *Polymer* 1985, 26, 177.
- (14) Deloche, B.; Beltzung, M.; Herz, J. *J. Phys. Lett. (Les Ulis, Fr.)* 1982, 43, 763.
- (15) Gronski, W.; Stadler, R.; Jacobi, M. M. *Macromolecules* 1984, 17, 741.
- (16) Toriumi, H.; Deloche, B.; Samulski, E. T.; Herz, J. *Macromolecules* 1985, 18, 305.
- (17) Ragle, G. L.; Sherk, K. L. *J. Chem. Phys.* 1966, 45, 3475.
- (18) This representation  $\Delta\nu$  vs.  $(\lambda^2 - \lambda^{-1})$  is well adapted here for two reasons: (i) the investigation is limited to the low-deformation regime; (ii) in the case of PDMS, a Mooney-Rivlin-like plot for the local ordering  $(\Delta\nu/(\lambda^2 - \lambda^{-1}) = D_1 + D_2/\lambda)$  is not useful since we always obtained  $D_2 = 0$ ; this is consistent with the fact that the constant  $C_2$  for the Young's modulus is known to be small for these materials (see, for instance: Valles, E.M.; Macosko, C. W. *Macromolecules* 1979, 12, 673).
- (19) For instance, it appears that the Young's modulus of end-linked polystyrene networks decreases of about 10% only for an increase of the fraction in dangling chains from 10% to 20% (see: Bastide, J.; Candau, S.; Picot, C. *J. Polym. Sci. Polym. Phys. Ed.* 1979, 17, 1441).
- (20) Deloche, B.; Dubault, A.; Herz, J.; Lapp, A. *Europhys. Lett.* 1986, 1 (12), 629.
- (21) We consider that the analysis based on  $\Phi_e$  are more relevant than those considering  $V_c$  because  $\Phi_e$  characterizes the final network whereas  $V_c$  is related to the cross-linking reaction only. Nevertheless, the observed proportionality of  $\langle P_2 \rangle$  as with  $\Phi_e$  or with  $V_c$  implies that for the PDMS studied here  $\Phi_e \propto V_c$ . But such a proportionality is not always true as it appears in ref 1.
- (22) Ball, R.; Doi, M.; Edwards, S. F.; Warner, M. *Polymer* 1981, 22, 1010.
- (23) Thirion, P.; Weil, T. *Polymer* 1983, 25, 609.
- (24) Edwards, S. F.; Vilgis, Th. *Polymer* 1986, 27, 483.
- (25) Dubault, A.; Ober, R.; Veyssie, M.; Cabane, B. *J. Phys. (Les Ulis, Fr.)* 1985, 46, 1227.

## Molecular Orientation and Structure in Solid Polymers with <sup>13</sup>C NMR: A Study of Biaxial Films of Poly(ethylene terephthalate)

P. Mark Henrichs

Corporate Research Laboratories, Eastman Kodak Company, Rochester, New York 14650.  
Received December 23, 1986

**ABSTRACT:** Two- and three-dimensional experiments greatly expand the applicability of <sup>13</sup>C NMR to measurement of molecular orientation in samples of synthetic polymers. For biaxially oriented films of poly(ethylene terephthalate) (PET) it has been possible to measure all orientation moments for which  $l = 2$ . There is a highly oriented component of the film for which the planes of the aromatic rings lie close to, but not in the plane of, the film. The protons in this component relax slowly in the rotating frame, suggesting that it largely comprises the crystalline portion of the film. The observed chemical shifts of the carbons in the film are adequately explained in terms of the known crystal structure of PET. A component of the sample whose protons relax rapidly in the rotating frame is much less oriented relative to the plane of the ring than is the crystalline portion. This component may be considered amorphous because the short proton relaxation time indicates that the polymer chains are relatively mobile.

## I. Introduction

Industrial processing of polymeric materials often induces a high degree of molecular orientation in the individual polymer chains.<sup>1</sup> This orientation can have both

positive and negative effects on the quality of the product.

For example, extrusion to produce fibers tends to orient the polymer chains along the extrusion direction. Much of the strength of extruded fibers is derived from the

molecular orientation because stretching of the drawn sample is opposed in large part directly by the strength of the chemical bonds holding the backbone together, rather than by chain entanglements or intermolecular forces.

Stretching of polymer films causes the polymer chains to lie in the plane of the film in the direction of stretch. Unoriented films often are relatively weak and brittle.<sup>3</sup> Production processes that yield a uniform distribution of chain directions within the plane of the film give optimum film strength. The time dependence of molecular orientation in polymer samples can also be important.

Above the glass-transition temperature, the molecules in an oriented polymer gradually relax back to random orientation,<sup>2,3</sup> but if the sample is cooled before the relaxation process is complete, the orientation may be preserved. The relaxation process can then be reactivated at some later time by heating. As a result, oriented materials often shrink with heating.<sup>3</sup> Products such as heat-shrinkable electrical insulation and bottle seals take advantage of the tendency of oriented polymers to shrink upon heating.

Even at temperatures below the glass transition, the dimensions of oriented samples may change slowly over long periods of time as the molecular orientation, particularly in the amorphous regions, relaxes. Long-term dimensional instability has practical consequences for certain applications of polymers. For example, it can limit the density of information that may be stored on magnetic tapes or disks.<sup>4</sup>

Many methods can be used to measure the degree of molecular orientation in solid polymers,<sup>1</sup> and a number of these have been applied to polyesters.<sup>5-11</sup> Techniques that give information selectively about molecular orientation in the crystalline or amorphous regions are especially valuable, however. Nuclear magnetic resonance (NMR) is one such method because nuclei in the crystalline regions of polymeric samples often relax at different rates from those of nuclei in the amorphous regions. In favorable cases, signals from one or the other of the two regions may be selected on the basis of the differences in relaxation rates. The next few paragraphs summarize some of the ways NMR can be used for orientation measurements.

Historically most orientation determinations with NMR have taken advantage of the angular dependence of the dipolar couplings among protons in the sample. So many protons are connected by dipolar coupling in the typical polymer sample, however, that the proton spectrum generally is broad and devoid of specific features. Detailed analysis of molecular orientation is often difficult, but proton NMR has given useful information about molecular orientation in some cases.<sup>12-16</sup>

The coupling of quadrupolar nuclei such as deuterium with the electric field gradient at the nucleus is a one-body, orientation-dependent interaction. As a result many of the complications of proton NMR are avoided if deuterium NMR is used for orientation measurements.<sup>17,18</sup> Deuterium NMR is restricted, of course, to samples that have been enriched isotopically with deuterium. Furthermore, the local environment around a C-D bond effectively has axial symmetry. The deuterium spectrum does not differentiate in molecular orientations differing only by rotation about the C-D bond.

Potentially, one of the most informative nuclear interactions is the anisotropic chemical shift,<sup>18-22</sup> especially for <sup>13</sup>C.<sup>23-27</sup> The chemical shift, like the quadrupole coupling, is a one-body interaction. Mathematically it is much simpler to treat than is the dipolar coupling interaction,

which involves two or more nuclei. Furthermore, local symmetry usually does not cause a loss of information as it does for deuterium NMR. Overlap of the signals from several different types of nuclei can be a problem, but as is shown below, there are experimental recourses to alleviate this difficulty.

The research described here was undertaken to explore new ways to measure orientation in biaxial films of an important industrial polymer, poly(ethylene terephthalate) (PET), with <sup>13</sup>C NMR. Numerous other studies of orientation in PET films provide a useful basis for calibration of the new methods.<sup>5-11,28-39</sup>

Several specific questions were addressed in the research. (1) Could the problem of spectral overlap of the bands from the various types of carbons in PET be overcome? (2) Could information about orientation in either the crystalline or amorphous regions of the sample be selected through manipulations of the relaxation properties of the spin system? (3) Could detailed mathematical information about the probability function describing molecular orientation be obtained? These questions will be addressed in more detail after the theoretical basis for the measurements has been established.

## II. Theoretical Section

**II.1. Axis Systems.** Defining the orientation in the sample of a given section of a polymer chain is equivalent to specifying the orientation of a coordinate system fixed in that fragment (the molecular axis system)<sup>40</sup> with respect to a coordinate system fixed in the sample (the sample axis system). Euler angles describing how the molecular axis system can be rotated into alignment with the sample axis system are useful for this purpose. We use the convention of Hentschel, Schlitter, and Spiess for the Euler angles.<sup>41</sup> The angle  $\alpha$  refers to rotation of the original axis system about its own  $z$ -axis, the angle  $\beta$  refers to rotation about the new  $y$ -axis, and the angle  $\gamma$  refers to rotation about the final  $z$ -axis.

In practice, the molecular and sample axis systems are not convenient for description of all aspects of experiments used to measure molecular orientation. It is helpful to define additional axis systems which are rotated from the molecular or sample axis systems. For example, the NMR chemical shift interaction for each nucleus is most simply described in a principle axis system (PAS) specific to that nucleus. The PAS for each nucleus usually has its own unique orientation with respect to the molecular axis system, as specified by a set of Euler angles  $\alpha_1$ ,  $\beta_1$ , and  $\gamma_1$ . The NMR phenomenon as a whole is best referred to in a frame fixed with respect to the direction of the magnetic field, usually taken as the  $z$  direction. This is the laboratory frame. Experimentally, the particular NMR spectrum obtained for an oriented sample is determined by the orientation of the sample axis system in the laboratory frame, specified by a set of Euler angles  $\alpha_2$ ,  $\beta_2$ , and  $\gamma_2$ .

In some of the experiments that will be described, the orientation of the sample was varied by rotation of it with a goniometer. It is convenient to define a goniometer frame having its  $z$ -axis aligned with the rotation axis. Rotation about that axis can then be described with a single Euler angle  $\alpha''$ . The overall orientation of the sample axis system with respect to the laboratory axis system can be decomposed into the orientation of the sample with respect to the goniometer frame, specified by Euler angles  $\alpha'$ ,  $\beta'$ , and  $\gamma'$ , and the orientation of the goniometer frame with respect to the laboratory frame, specified by Euler angles  $\alpha''$ ,  $\beta''$ , and  $\gamma''$ . The overall scheme is shown in Figure 1.

We will have occasion to use several different definitions

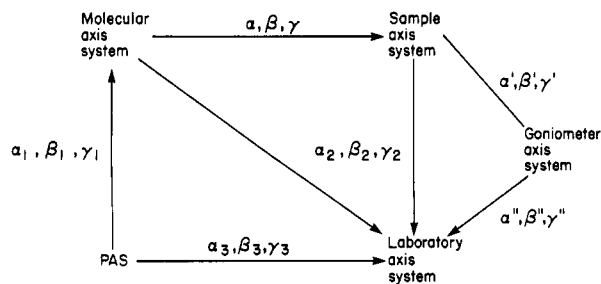


**Figure 1.** Coordinate systems used in the analysis of molecular orientation. Euler angles are given above the arrows to describe the rotation from one axis system to another.

of the molecular axis system. In each of these the molecular coordinates of the individual nuclei will be different. For the moment, we will continue to refer to the molecular axis system in a generic sense, leaving specific definitions to the Discussion.

**II.2. Orientation Moments.** Ideally, the experimental results should lead, with appropriate analysis, to a distribution function  $P(\Omega)$  describing the probability that the molecular axis system of an arbitrarily chosen polymer fragment can be rotated into alignment with the sample axis system with the set of Euler angles represented by  $\Omega$ . Commonly,  $P(\Omega)$  is expanded into an infinite series<sup>41-48</sup> on the basis of functions such as the elements of the Wigner rotation matrices<sup>49</sup> (or equivalent functions such as generalized spherical harmonics). For the expanded function, the coefficients  $P_{lmn}$  are the parameters that have to be determined experimentally.

In terms of the rotation matrix elements

$$P(\Omega) = \sum_{lmn} P_{lmn} D_{mn}^l(\Omega) \quad (1)$$

where  $P_{lmn} = [(2l+1)/(8\pi^2)] \int D_{mn}^l(\Omega) d\Omega$ . Because the coefficients  $P_{lmn}$  often become quite large for large values of  $l$ , it is convenient to define a second set of functions  $\hat{P}_{lmn} = [8\pi^2/(2l+1)] P_{lmn}$ . In this paper these functions will be referred to as the "orientation moments".<sup>50</sup>

The functions  $D_{mn}^l(\Omega)$  have the form  $e^{-iam} d_{mn}^l(\beta) e^{-i\gamma n}$ . Symmetry in either molecule or the sample causes the weighted average over these functions to disappear for some values of  $l$ ,  $m$ , and  $n$ .<sup>51</sup> For example, if there is a uniform distribution of the molecules about the  $z$ -axis of the sample axis system,  $P(\Omega)$  is independent of the angle  $\gamma$ . We see that the moments vanish unless  $n = 0$ . Likewise, if there is axial symmetry about the  $z$ -axis in the molecular axis system, nonzero moments must have  $m = 0$ . The complete symmetry properties of the Wigner rotation matrix elements allow the treatment of other cases of symmetry.<sup>41</sup>

If both the sample and the molecule have three mutually perpendicular planes of symmetry (orthorhombic symmetry), all orientational moments for which  $l$ ,  $m$ , and  $n$  are odd have the value zero.<sup>53</sup> Furthermore, the expansion moments are all real, and  $\hat{P}_{lmn} = \hat{P}_{lm-n} = \hat{P}_{l-mn} = \hat{P}_{l-m-n}$ . For practical purposes in this case only moments with positive values of  $m$  and  $n$  need to be measured experimentally.

Biaxially oriented samples do have three mutually perpendicular planes of symmetry. The local orienting units of PET probably do not. Nevertheless, we will assume that the distribution of orientations for these units is close to that which would occur if they had three orthogonal planes of symmetry. This assumption is not justifiable in the strictest sense but does simplify the calculations considerably.

Assumption of biaxial symmetry in both the sample and the orienting molecular fragment allows us to concentrate on the moments derived from only a few of the Wigner matrix elements. The mathematical form for these is

$$\hat{P}_{200} = \frac{4\pi^2}{5} \langle 3 \cos^2 \beta - 1 \rangle$$

$$\hat{P}_{202} = \frac{4\pi^2}{5} \frac{3}{2} \langle \sin^2 \beta \cos 2\gamma \rangle$$

$$\hat{P}_{220} = \frac{4\pi^2}{5} \frac{3}{2} \langle \sin^2 \beta \cos 2\alpha \rangle$$

$$\hat{P}_{222} = \frac{4\pi^2}{5} \langle (1 + \cos^2 \beta) \cos 2(\alpha + \gamma) - 2 \cos \beta \sin 2(\alpha + \gamma) \rangle$$

$$\hat{P}_{400} = \frac{8\pi^2}{9} \langle 35 \cos^4 \beta - \cos^2 \beta + 3 \rangle$$

The functional form of other moments is available in the literature.<sup>53</sup>

**II.3. Orientation Measurements with NMR Spectroscopy.** Most experimental techniques give information about only a few of the expansion terms in eq 1.<sup>43,44</sup> For example, infrared dichroism relates only to those moments with  $l = 2$ ; fluorescence polarization can be used to derive moments with  $l = 0, 2$ , or  $4$ . In principle, all of the orientation moments can be obtained with X-ray diffraction, but X-ray analysis is not suitable for examination of molecular orientation in the amorphous regions of polymers, and other methods are still helpful for use in conjunction with it.

NMR spectroscopy is capable of giving, theoretically, all of the orientation moments with  $l$  even, but experimental factors limit the number of moments that can be found in practice.<sup>1</sup> Analysis of proton spectra that have been broadened by dipolar coupling is particularly restricted. Only in drawn polyethylene have the orientation moments  $\hat{P}_{100}$  with  $l$  as large as 6 been determined from the proton NMR spectra.<sup>54</sup> The advantage of the chemical-shift anisotropy as an alternative source of information is illustrated by the fact that, in drawn poly(tetrafluoroethylene), moments where  $l$  has even values up to 8 have been extracted from the spectra broadened by the fluorine chemical-shift anisotropy.<sup>19-22</sup> Still, the samples that had been treated previously were highly symmetrical; NMR has not been used for analysis of biaxially oriented samples, for which a relatively large number of moments must be found.

Let us now consider how molecular orientation determines the chemical shift. The mathematical entity of interest is the chemical-shift tensor **A**. In the laboratory frame, the observed chemical shift of a particular nucleus is given by the element  $A_{zz}$  of the chemical-shift tensor.<sup>55</sup>

In general, the chemical-shift tensor in a frame rotated from the PAS must be determined from the tensor in the PAS with a unitary transformation

$$\mathbf{A}' = \mathbf{R} \mathbf{A} \mathbf{R}^{-1} \quad (2)$$

where **R** is a matrix for rotation of Cartesian coordinates. The elements of **R** should not be confused with the Wigner rotation matrix elements, whose elements are used for expansion of the orientational distribution function.

Through a sequence of unitary transformations the chemical-shift tensor in any of the axis systems in Figure 2 can be found if the elements of the tensor in the PAS are known. If the Euler angles for direct rotation of the

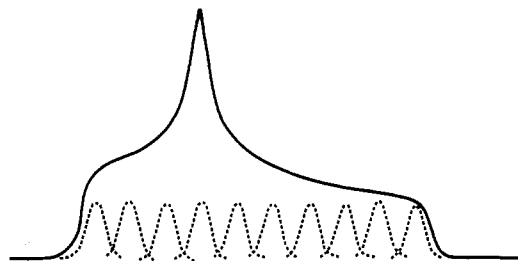


**Figure 2.** Generalized powder lineshape resulting from the chemical-shift anisotropy. The observed band is a superposition of many components, indicated by the dotted lines, each of which may correspond to several molecular orientations.

PAS to the lab frame are available, however, the chemical shift is given by

$$A'_{zz} = A_{xx} \cos^2 \beta_3 \sin^2 \alpha_3 + A_{yy} \sin^2 \beta_3 \sin^2 \alpha_3 + A_{zz} \cos^2 \beta_3 \quad (3)$$

where  $A_{xx}$ ,  $A_{yy}$ , and  $A_{zz}$  are the principle elements in the PAS and  $\alpha_3$  and  $\beta_3$  are the Euler angles required for rotation of the PAS into the laboratory frame. The Euler angle  $\gamma_3$  is irrelevant because rotation of the sample about an axis parallel to the magnetic field does not change the chemical shift.

In a powder the molecules are oriented randomly. The observed spectrum is the superposition of the signals from molecules having all possible orientations. A typical spectrum from a single type of nucleus is shown in Figure 2. In an oriented sample, molecules with certain orientations are absent. The observed spectrum is more intense in some regions and less intense in others than is the spectrum in Figure 2. Furthermore, the shape of the spectrum depends on the orientation of the sample in the magnetic field.

Although the NMR spectrum of each nucleus in an oriented material usually deviates from the shape shown in Figure 2, the simple NMR spectrum cannot generally be used directly as a basis for determination of the complete orientation distribution function. Only in the case in which there is axial symmetry in both the molecule and the sample is the spectral intensity at any given frequency directly proportional to the population of molecules in a particular orientation. Even in this case the NMR spectrum does not differentiate between molecules that differ in orientation only by rotation about the direction of the magnetic field (as specified by the Euler angle  $\gamma_3$ ). In addition, several different combinations of the angles  $\alpha_3$  and  $\beta_3$  in eq 3 can give rise to the same chemical shift.<sup>56</sup>

Complete solution of the orientation problem requires examination of the NMR spectra for several different orientations of the sample in the spectrometer. In fact, analysis of rotation plots of the chemical shift is the standard method for determination of the principle elements and orientation of interaction tensors in magnetic resonance. Rotation plots are usually determined for single crystals of relatively simple molecules, however. For each orientation of the sample there are only a few NMR resonances. The change in frequency of each resonance as the sample is rotated is easily determined. For a partially oriented polymer there is a continuous distribution of spectral components. Special methods are necessary if the changes of these spectral components with rotation of the sample are to be followed.

Recently developed pulse sequences allow direct correlation of the spectral components for one orientation with those for another.<sup>57-59</sup> The orientation of the sample is changed in a dynamic fashion during the course of a single NMR experiment. The scheme is sketched in Figure 3a.

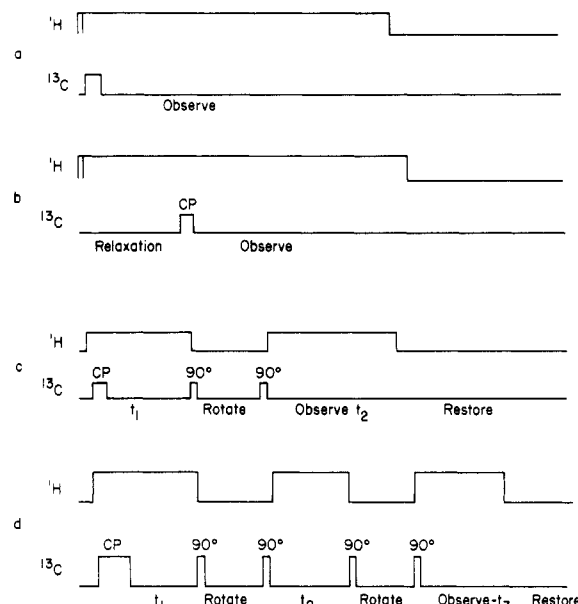


**Figure 3.** Pulse sequences used to generate  $^{13}\text{C}$  NMR spectra: (a) standard cross polarization; (b) proton relaxation in the rotating frame followed by cross polarization; (c) sequence to generate two-dimensional spectra with sample rotation; (d) sequence to generate three-dimensional spectra with sample rotation.

Transverse magnetization is initially created by cross polarization. The magnetization is then allowed to evolve in the rotating frame for time  $t_1$ . The evolution frequency of each magnetization component (see Figure 1) is determined by the orientation of the particular molecule associated with the magnetization component.

At the end of  $t_1$  a portion of the transverse magnetization is converted into longitudinal magnetization by application of a  $90^\circ$  pulse. A given transverse magnetization component is completely converted into longitudinal magnetization only if it is perpendicular to the direction of the effective field in the rotating frame at the time of the pulse. Its actual orientation is controlled by the time development during  $t_1$ . Thus, the amplitude of longitudinal magnetization resulting after the pulse reflects the evolution frequency during  $t_1$ .

Following the  $90^\circ$  pulse, there is ample time for rotation of the sample before significant longitudinal magnetization is lost because spin-lattice relaxation for  $^{13}\text{C}$  nuclei in most polymers occurs on a time scale of seconds and sample rotation can be accomplished in times less than 200 ms. A second  $90^\circ$  pulse after rotation is finished recreates transverse magnetization, each component of which evolves in time at a frequency determined by the second orientation of the molecule associated with it.

Fourier transformation of the two-dimensional data from an experiment performed as described in the previous paragraph yields a spectrum that correlates frequencies for two different orientations of the sample.<sup>60</sup> This spectrum is not yet adequate for complete solution of the orientation problem, however. Several different molecular orientations can still give rise to intensity in the two-dimensional spectrum at the same pair of frequencies. A three-dimensional NMR spectrum correlating spectral frequencies for three different sample orientations is necessary.

A tempting approach to obtaining the three-dimensional data would be generation of a set of three two-dimensional spectra correlating the spectral frequencies for three different pairs of sample orientations. This approach is not, in fact, adequate for calculation of the full three-dimensional spectrum. Assume that the frequencies have been

partitioned into  $n$  channels. The three-dimensional matrix of data needed contains  $n^3$  elements. But three two-dimensional matrices contain only  $3n^2$  elements. As long as more than three frequency channels are used, the two-dimensional spectra do not contain enough information for calculation of the full three-dimensional spectrum.

There is a special case in which a set of two-dimensional spectra would be sufficient for solution of the orientational problem, however. The full spectrum for any one orientation of the sample is a superposition of the resonances for all orientations of the molecular axis system relative to the sample axis system which are present. If the number of orientations is limited such that the spectral components are resolved for all three orientations of the sample, the full three-dimensional spectrum provides no additional information over several two-dimensional spectra. In fact, when each spectrum contains only a few signals, a set of one-dimensional spectra suffices. It is the wide range of molecular orientations present in most polymer samples that mandates the need for multidimensional NMR whereas a plot of chemical shift vs. chemical shift in a rotation plot is enough for a single crystal. The three-dimensional NMR spectrum for determination of the probability distribution function can be generated by extension of the pulse sequence for the two-dimensional spectrum (Figure 3b).

Interconversion from one sample orientation to another is most easily achieved by rotation about a single axis. This axis is the  $z$  direction in the goniometer axis system. Experimentally it is simplest to place the goniometer axis perpendicular to the direction of the magnetic field and to orient the sample with one of its symmetry axes parallel to the goniometer axis. The three sample orientations may be chosen to differ by rotations of  $45^\circ$  about the goniometer axis.

That molecules having different orientations with respect to the sample (as defined by the Euler angles  $\alpha$ ,  $\beta$ , and  $\gamma$ ) do differ in NMR frequencies for at least one of the three sample orientations in the arrangement described in the previous paragraph can be verified with eq 2. In fact, two molecules whose orientations differ by  $\pi$  in  $\alpha$  or by  $\pi$  in  $\gamma$  do have the same set of frequencies. The assumptions of orthorhombic symmetry in the sample and molecule require the abundance of molecules whose orientations differ in this fashion to be equal, however. Rotation about the axis perpendicular to the magnetic field completely removes the degeneracy in NMR frequencies for orientations not related by symmetry.

Once an appropriate three-dimensional NMR spectrum has been measured, the orientational moments must be determined from it. A useful approach involves the calculation of a number of three-dimensional "subspectra", each one of which is associated with one of the Wigner rotation matrix elements. Subspectra may be calculated numerically in the same fashion as is a standard powder pattern by collecting spectral components at equivalent frequencies as the molecular orientations are systematically varied over all possible values.<sup>61</sup> The spectral contribution from each molecular orientation is weighted, however, by the corresponding value of the appropriate Wigner rotation matrix elements. These subspectra are not realistic in the sense that they contain negative as well as positive frequencies, but the expansion coefficients in eq 1 can be found simply by determining the combination of subspectra that adequately reproduces the experimental spectrum. The procedure for simulation of three-dimensional spectra is identical with that developed by Spiess and co-workers for analysis of one-dimensional deuterium

spectra of oriented materials.<sup>41</sup>

Clearly it is not possible to determine an unlimited number of orientation moments from an actual experimental spectrum. There are several practical limitations. Intensity in the subspectra based on the elements of the Wigner rotation matrix elements oscillates between positive and negative values, the number of oscillations increasing as the indices increase in size. A given orientational moment can be found only if the period of the oscillations within the corresponding subspectrum exceeds the effective resolution within the NMR spectrum. In the three-dimensional spectrum digital resolution is likely to be the limiting factor. Unless the expansion series for the distribution function converges rapidly, the signal-to-noise ratio of the spectrum will also interfere with the determination of smaller moments. An important goal of the present research was to determine experimentally where the practical limitation in measurement of orientational moments lies.

### III. Experimental Section

**III.1. Sample Preparation.** Films of poly(ethylene terephthalate) were supplied by R. W. Schrader, of the Materials Science and Engineering Department, Eastman Kodak Company. Most measurements were made from a production sample of Kodak Estar film base. Estar base is a trademark to identify Kodak's version of a biaxially oriented polyester film stretched in the longitudinal (machine) direction and then in the transverse (tentering) direction. The polymer chains are oriented to a slightly greater extent in the tentering direction than in the machine direction.

NMR measurements were made on stacked strips measuring 7 by 15 mm. The strips were sealed at the ends with a small drop of cyanoacrylic adhesive and were held in the spectrometer in notched glass rods. Because the amount of glue used was small, it is not expected to contribute significantly to the observed spectra.

**III.2. NMR Spectra.** A Bruker CXP-100 spectrometer with a wide-bore superconducting magnet was used for all measurements. All spectra were generated with the cross-polarization technique with contact times of 1 ms. Pulse times required to rotate either the carbon or proton magnetization through  $90^\circ$  were about 4  $\mu$ s. The spectrometer was carefully adjusted to minimize software phase corrections by precise setting of the phase of the reference signal going into the phase detector and optimization of the delay between the end of the cross-polarization procedure and the beginning of data acquisition.<sup>62</sup> Base-line rolls in the spectra were corrected by simulation either as a first-order polynomial or as a sum of sine and cosine functions.

Two-dimensional spectra were generated with the standard software supplied by Bruker Instruments, Inc., and with routines written in the computer language Pascal. Phase-sensitive, multidimensional spectra were created by zeroing the imaginary portion of the spectrum following the first transformation step. This method destroys information about the sign of the frequencies in the higher dimension and thus requires selection of a spectrometer frequency to one side of the region of interest. The spectra shown in the figures are from a single quadrant of  $64 \times 64$  real points from the final spectrum, the other quadrants being redundant. The one- and two-dimensional spectra were processed with 100 Hz of Lorentzian broadening.

Three-dimensional spectra were generated from a set of free-induction signals measured as a function of  $t_3$ , each one containing 512 words of real and imaginary data and corresponding to one of the various combinations of  $t_1$  and  $t_2$  values. The free-induction decay signals were multiplied with an exponential corresponding to 400 Hz of line broadening and then were Fourier transformed. A minor phase correction was made, and base-line roll was simulated with a first-order polynomial and removed. Every fourth point was then collected into a smaller data set for further processing.

Points in the reduced data set were then interchanged with a Pascal routine to create a set of functions of  $t_2$ , each corresponding to a frequency  $\nu_3$  and a time  $t_1$ . The imaginary portions

of these signals were set to zero before Fourier transformation and processing as before. The results were transposed to give a set of functions of  $t_1$ , which were further processed to give the desired set of data as a function of three frequencies. Only a single octant of the full spectrum was retained because, with the zeroing of the imaginary portions of data before the Fourier transformations, the other quadrants were redundant.

The final results were arranged with another Pascal program into a set of two-dimensional spectra. Each two-dimensional spectrum was a slice from the full spectrum, which could be displayed and plotted with the standard software on the Bruker Aspect computer.

To allow the sample to be rotated, the NMR probe was modified by addition of a stainless-steel (nonmagnetic) shaft attached to a worn gear. Rotation was controlled by a stepping motor driven by a home-built device triggered from a pulse of the spectrometer pulse program. Rotation through an angle of  $90^\circ$  required 40 ms, followed by 100 ms to allow dissipation of vibration in the probe coil before the next excitation pulse. During this period transverse carbon magnetization irreversibly decays. No significant longitudinal relaxation was observed during the time of rotation. The phases of the pulses used to store magnetization during the rotation were alternated to eliminate artifacts. The initial orientation of the sample was set by eye so that the film was perpendicular to the magnetic field. The error in doing this is estimated to be less than  $5^\circ$ .

**III.3. Computer Calculations.** Computer simulations were made on a IBM 3090 mainframe computer with programs written in FORTRAN. The program for calculation of subspectra allows for input of an assumed molecular structure, principle elements, and orientation of the PAS for each nucleus relative to the assumed molecular axis system, the orientation of the sample axis system relative to the axis of the isolation, and the three angles of rotation about this axis for the three-dimensional experiment. The input parameters actually used are described in the text.

The Euler angles describing the orientation of the molecular axis system with respect to the sample axis system were systematically varied over all possible values by the program. For each molecular orientation the chemical shifts associated with the three sample orientations in the experiment were calculated with the help of eq 2 for all carbons in the molecule. The intensity at the appropriate set of frequencies in each subspectrum for that orientation was then given the value of the appropriate Wigner rotation matrix element. The elements themselves were calculated from those for  $l = 2$  on the basis of the well-known expansion formula.<sup>49</sup> The intensities of all the signals falling within a given unit volume of the three-dimensional spectrum were summed to give the complete spectrum.

Calculated subspectra were convoluted with a Lorentzian function, a Gaussian function, or both to provide suitable data for spectral simulation. The experimental spectra were reduced to 16 frequency channels in each dimension for fitting to the experimental data. The simulation itself was done with a standard least-squares fitting routine. Optimal fit resulted from Lorentzian broadening of 400 Hz combined with Gaussian broadening of 1000 Hz. An almost equally good fit occurred with 600 Hz of Lorentzian broadening only.

## IV. Results

**IV.1. PET Powder.** The one-dimensional  $^{13}\text{C}$  spectrum of a semicrystalline powder of poly(ethylene terephthalate) is shown in Figure 4a. Previously reported spectra of PET are similar, the principal differences lying in the band on the right assigned to the methylene carbons.<sup>63,64</sup> The gauche conformation of PET occurs only in the amorphous portion of the sample.<sup>30,65-70</sup> We may expect that the NMR spectra of the gauche and trans conformations will differ primarily in the signals of the methylene carbons. Thus, variations in the spectra of different samples can largely be accounted for by differences in the degree of crystallinity of the samples.

It is desirable to determine separately the molecular orientation in the crystalline and amorphous domains of polyester films. Various schemes taking advantage of

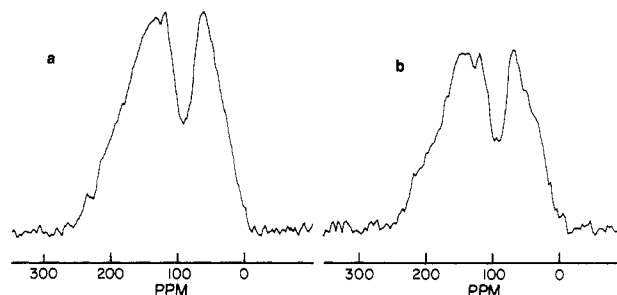


**Figure 4.**  $^{13}\text{C}$  spectra of a semicrystalline powder of poly(ethylene terephthalate): (a) acquired with standard cross polarization (Figure 2a); (b) acquired following relaxation of proton magnetization in the rotating frame for 30 ms prior to cross polarization (Figure 2b).

differences in the relaxation properties of either the protons or carbons in the two regions might allow this.<sup>71</sup> Possible orientation dependence of the nuclear relaxation times can complicate the choice of an appropriate method, however.<sup>72,73</sup> One way to check whether a given scheme selects signals primarily on the basis of whether the nuclei are in crystalline or amorphous regions or primarily on the basis of the orientation of the molecules containing the nuclei is to apply it to the randomly oriented powder. If the selection is largely independent of molecular orientation, the spectrum with the special pulse scheme should be the same as that taken under normal conditions.

For PET powder pulse schemes selecting signals on the basis of differences in carbon relaxation times gave very different spectra from those provided by the standard cross-polarization procedure. The relaxation times of the carbons appear to have a significant orientation dependence. On the other hand, schemes selecting carbon signals on the basis of differences in proton relaxation times gave spectra that were almost identical with those obtained in the standard manner. Figure 4b shows one such spectrum, in which the spin-locked proton magnetization was held for 30 ms prior to cross-polarization transfer from the protons to the carbons. Havens and VanderHart have shown that relaxation of spin-locked proton magnetization can be decomposed into a fast component with a relaxation time of about 5 ms and a slow component with a relaxation time of 20–40 ms.<sup>74</sup> To the extent that the slow component of proton relaxation is associated with crystalline regions of the sample, the spectrum in Figure 4b is largely that of the crystalline regions.

Analysis of the spectra of oriented materials requires interpretation of the spectra in Figure 4 in terms of the patterns for the individual types of nuclei in the sample. Gerstein and co-workers have decomposed the spectrum by experiments involving spinning about axes oriented with respect to the magnetic field at angles slightly different from the magic angle.<sup>63</sup> The bands for each type of carbon are narrowed but are not collapsed into sharp spikes in this experiment. The individual, narrowed shapes can be analyzed in terms of the chemical shift anisotropy without the problem of severe signal overlap. Later work by VanderHart provides more refined values for the principal elements of the chemical shift tensors and forms the basis for the analyses in this paper.<sup>75</sup> The chemical shifts are summarized in Table I.

**IV.2. Biaxial Kodak Estar Films. IV.2.1. One-Dimensional NMR Spectra.** Spectra for three orientations of the PET films in the magnetic field appear in Figure 5. The spectra on the left were taken with the standard cross-polarization method; the spectra on the right were acquired after the protons were allowed to relax partially in the rotating frame.



**Table I**  
Assumed Principal Values of  $^{13}\text{C}$  Chemical Shifts for Poly(ethylene terephthalate)<sup>a</sup>

	$\omega_{xx}$	$\omega_{yy}$	$\omega_{zz}$
proton-bearing aromatic	223	159	11
proton-free aromatic	230	145	26
carbonyl	252	131	107
methylene	87	75	20

<sup>a</sup>Based on personal communication by D. L. VanderHart. In ppm from liquid tetramethylsilane.

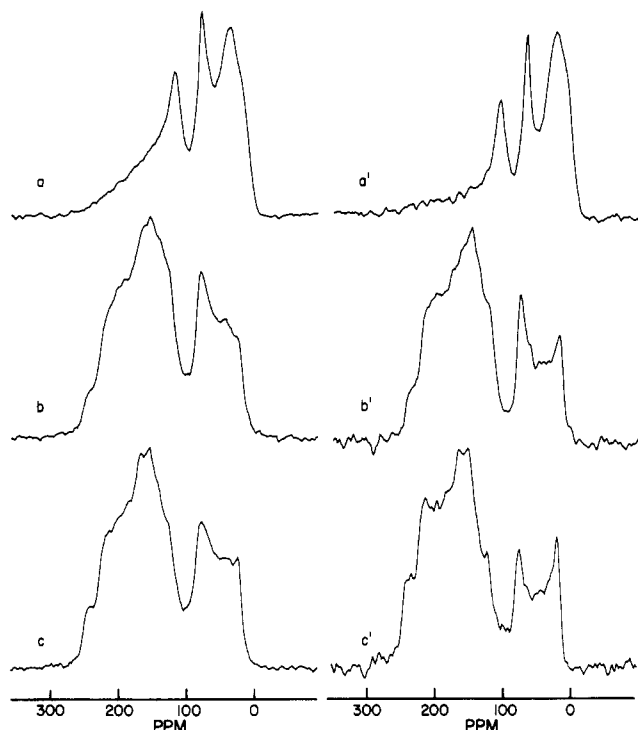


**Figure 5.** One-dimensional  $^{13}\text{C}$  NMR spectra of biaxially oriented films of poly(ethylene terephthalate): (a) film oriented perpendicular to the magnetic field; (b) and (c) film oriented with symmetry axes parallel to the direction of the magnetic field. The spectra on the left were acquired with standard cross polarization as shown in Figure 2a. The spectra on the right were taken after proton relaxation in the rotating frame in the scheme of Figure 2b for 20 ms.

Film oriented perpendicular to the field gave the simplest spectrum, as shown by Figure 5a. Essentially, there are three bands superimposed on a broad background signal. The sharp signals may be assigned to the carbonyl, aromatic, and methylene carbons with the help of Table I. Only the leftmost signal falls within the range possible for carbonyl carbons, for example. The peak on the far right has the greatest integrated intensity and is assigned to the aromatic carbons. There is an incipient splitting as a result of the fact that there are three different types of aromatic carbons in PET. The peak in the center comes from the methylenes.

The sharpness of the signals suggests that there is a high degree of uniformity in the way most of the molecules are oriented with respect to the film plane. A significant portion of the sample is disordered as well, however, as shown by the broad background signal underneath the sharp peaks. This background signal is suppressed when the spin-locked proton magnetization is allowed to relax for 20 ms prior to cross polarization, as may be seen in Figure 5a'.

The spectra in Figure 5b,c were obtained for two orientations of one of the symmetry axis in the film plane parallel to the magnetic field. In (b) the machine direction

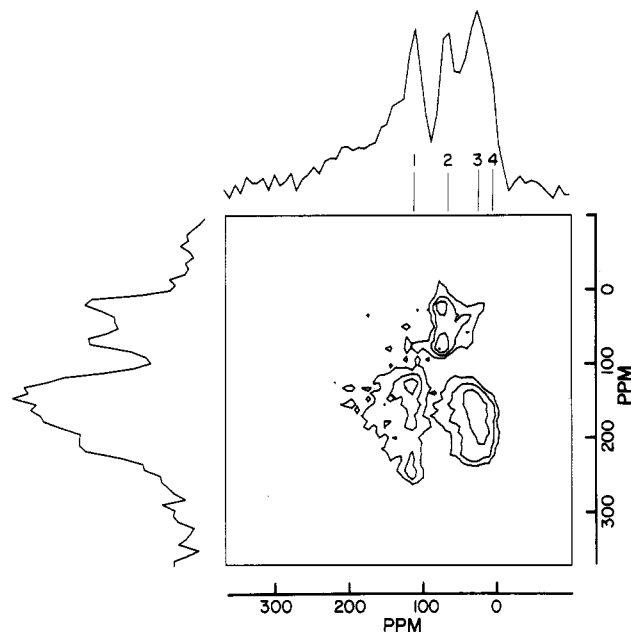


**Figure 6.** Two-dimensional spectrum correlating frequencies in the spectrum in Figure 4a with those in the spectrum of Figure 4b. Also shown are summation spectra for the two orientations.

was parallel to the field; in (c) the tentering direction was parallel. The spectra are very similar, but careful comparison shows differences in the intensities of a number of the shoulders. The differences are enhanced in the spectra obtained after partial relaxation of the proton magnetization (Figure 5b',c'). The skewing of the methylene region to the right in Figure 5c' is particularly noticeable.

Consistently in the one-dimensional spectra a small feature appears between 20 and 40 ppm. The origin of this signal is unclear, but English has observed a peak in the same region for samples of unannealed PET.<sup>64</sup>

**IV.2.2. Two-Dimensional NMR Spectra.** Analysis of orientation in PET films in terms of the NMR spectrum is complicated by the fact that the most resolved spectrum (Figure 5a) contains no information about the distribution of the polymer chains within the plane of the film; molecules differing in orientation only by rotation about an axis parallel to the direction of the magnetic field give the same NMR spectrum. Overlap of the signals from the aromatic and carbonyl carbons in Figure 5b,c interferes with an analysis of those spectra in terms of the distribution of the polymer chains within the film plane. Multidimensional spectra are needed to increase the amount of information available for analysis.

Figure 6 contains a contour plot of a two-dimensional spectrum taken with the pulse sequence in Figure 3c. The two sample orientations used in the experiment correspond to those used for Figure 5a,b. Summation of the two-dimensional spectrum to the horizontal axis and to the vertical axis do, in fact, reasonably reproduce the one-dimensional spectra although the methylene region is resolved into two peaks in the two-dimensional spectrum. The bands for the carbonyl and aromatic carbons, which overlap in the one-dimensional spectrum in Figure 5b, are clearly resolved in the two-dimensional spectrum.

The additional information provided by the two-dimensional spectrum can be seen more easily in slices (Figure 7) taken at the four positions indicated by vertical lines in Figure 6. The skewed doublet for the methylene carbon in the one-dimensional spectrum in Figure 5b appears distinctly in slice 2. Slice 1 containing the carbonyl signal also shows a skewed doublet. This feature is ob-

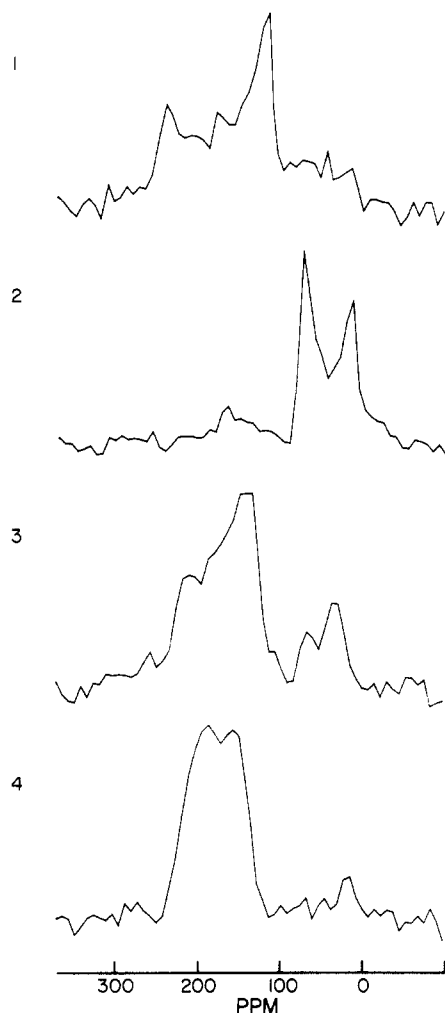


**Figure 7.** One-dimensional slices from the two-dimensional spectrum shown in Figure 5 taken perpendicular to the horizontal axis at the positions shown in Figure 6.

scured by peak overlap in the one-dimensional spectrum.

Figure 8 shows a contour plot of a two-dimensional spectrum correlating the one-dimensional spectra in Figure 5a,c. Slices at the same positions as those in Figure 7 appear in Figure 9. The skewing of the doublet in slice 2 of Figure 9 is in the opposite sense to that in slice 2 in Figure 6. In slice 1 of both figures the doublet is skewed in the same direction but to a much smaller degree in Figure 9 than in Figure 7.

**IV.2.3. Three-Dimensional NMR Spectra.** Although the two-dimensional NMR spectra provide more clear-cut information about molecular orientation in PET films than do the one-dimensional spectra, they do not provide a basis for complete quantitative evaluation. The three-dimensional spectrum corresponding to the three sample orientations used to generate Figure 5 would be impractical to generate.<sup>76</sup> Three-dimensional data were actually acquired with the sample rotated 0°, 45°, and 90° about a single axis perpendicular to the direction of the magnet field. In the 0° position the film plane was perpendicular to the magnetic field. The 90° position corresponded to that for the spectrum of Figure 5b. As was explained in the Theoretical Section, an experiment of this type is adequate for analysis of orientation of orthorhombic molecules in a sample with orthorhombic symmetry.

It is, of course, difficult to portray pictorially the entire three-dimensional spectrum. Two-dimensional slices corresponding to the one-dimensional slices in Figures 7 and 9 are shown in Figure 10. These slices are perpen-

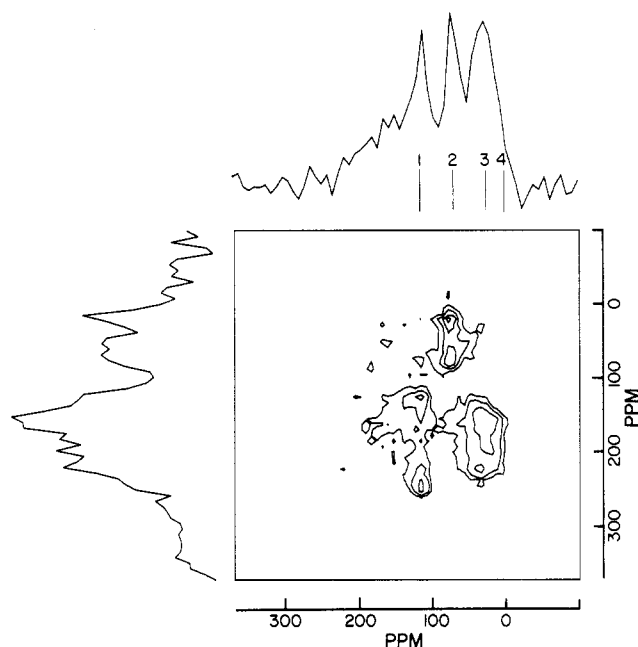


**Figure 8.** Two-dimensional spectrum correlating frequencies in the spectrum in Figure 4a with those in the spectrum of Figure 4c.

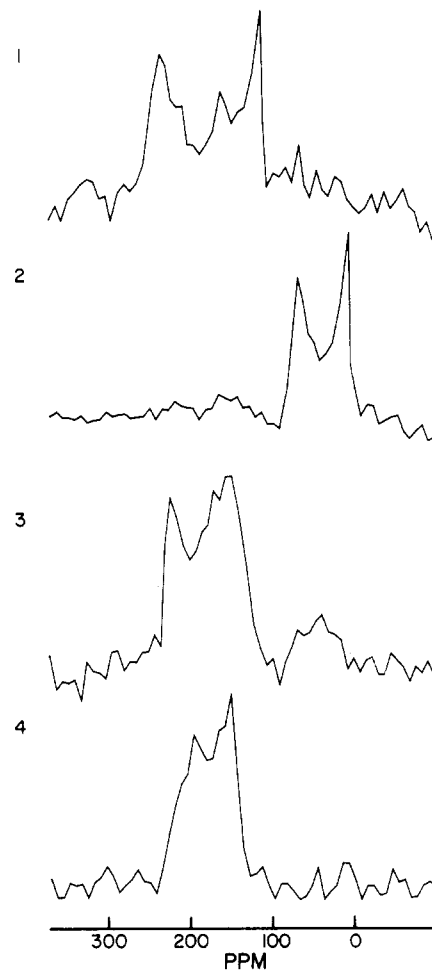


**Figure 9.** One-dimensional slices from the two-dimensional spectrum shown in Figure 7 taken perpendicular to the horizontal axis at the positions shown in Figure 8.

dicular to the spectral coordinate corresponding to the orientation of the film plane perpendicular to the magnetic field. Chemical shifts measured along the horizontal axes represent the sample frequencies for the 45° orientation.



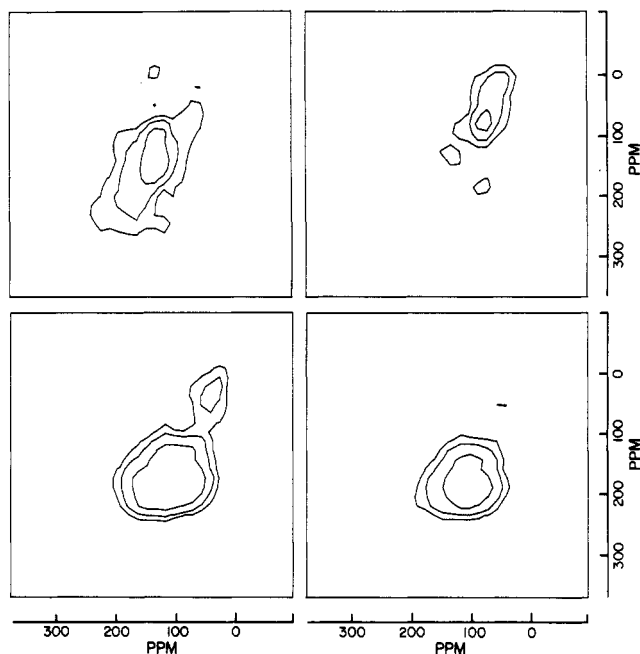


**Figure 10.** Two-dimensional slices from the three-dimensional rotation spectrum of polyester film. The slices correspond to the one-dimensional spectra shown in Figures 6 and 8.

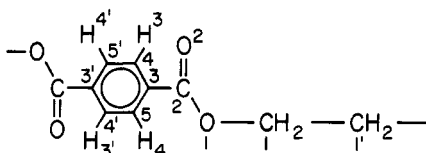


**Figure 11.** Numbering of the atoms whose coordinates are given in Table II. Carbons, oxygens, and hydrogens are numbered separately. The numbering follows that of Cunningham, Manuel, and Ward.<sup>78</sup> Note that C4 and C5 are inequivalent in the crystal.

Chemical shifts along the vertical axis relate to the orientation of the tenting direction parallel to the magnetic field.

Further spreading of the intensities in the two- and one-dimensional spectra is apparent in the three-dimensional spectrum. No new qualitative information is provided, however. The value of the three-dimensional spectrum is that it provides a basis for mathematical analysis.

## V. Discussion

**V.1. Basis of the Analysis. V.1.1. Molecular Structure.** The structure in the crystalline regions of the trans conformation of PET is known from X-ray diffraction<sup>77</sup> and was used in a modified form<sup>78</sup> for all computations. Atomic coordinates adapted from Cunningham, Manuel, and Ward (with the numbering system in Figure 11) are shown in Table II. The coordinate system used for Table II is the molecular axis system for most calculations. Alternative choices of the molecular axis system will be defined later.

Two major assumptions are involved in the use of the X-ray structure. (1) The trans conformation has the same structure in both the crystalline and amorphous regions. (2) The gauche conformation can be ignored. The second assumption requires special justification. The gauche conformation is certainly present in the PET film, although it is limited to amorphous regions. The structure of the gauche conformation presumably differs from the trans conformation primarily in the ethylene glycol portion of the molecule, however. The chemical shifts of the ethylene glycol carbons have the smallest orientation de-

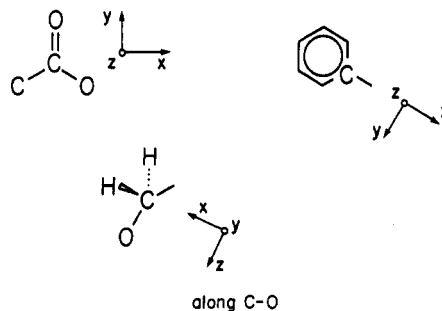


**Figure 12.** Orientations assumed for the chemical-shift tensors of the carbon nuclei in PET. The principal values associated with the three axes are shown in Table I.

**Table II**  
Atomic Coordinates Assumed for Trans PET in Molecular Axis System A

atom	x	y	z
H1	-1.481	0.160	0.284
H3	1.546	-0.228	3.514
H3'	-1.546	0.228	7.236
H4	-2.354	0.498	4.974
H4'	2.354	-0.498	5.776
C1	-0.430	0.435	0.408
C1'	0.430	-0.435	-0.488
C2	-0.916	0.541	2.707
C3	-0.395	0.233	4.057
C3'	0.395	-0.233	6.693
C4	0.860	-0.105	4.345
C4'	-0.860	0.105	6.405
C5	-1.300	0.297	5.131
C5'	1.300	-0.297	5.619
O1	-2.100	0.845	2.402
O2	0.000	0.209	1.770

pendence of any of the carbons in PET; the molecular orientation measured is thus largely the average orientation of the unit composed of the aromatic ring and carbonyl groups of both the trans and gauche conformations. At any rate the gauche conformation should be a minor component in the films and should contribute less intensity to the NMR spectrum than does the trans conformation.

**V.1.2. Chemical-Shift Tensors.** The orientation of the PAS for each carbon relative to the molecular axis system was assumed primarily to reflect the local structure of the polymer near the carbons. For example, in a variety of aromatic compounds the ring carbon is most shielded when the magnetic field is perpendicular to the aromatic ring.<sup>55,62</sup> The PAS orientation shown in Figure 12 was thus assumed. Carbonyl groups also appear to be most shielded when the magnetic field is perpendicular to the plane of the carbonyl group.<sup>62</sup> The direction of least shielding was assumed to lie along the CO bond.

The appropriate orientation for the PAS of the methylene carbons is subject to more uncertainty than is that for the other carbons, but in methanol the direction of most shielding is along the CO bond. The PAS for the methylene carbons in PET was also assumed to have the z-axis along the X bond. The orientation of the other two principal axes was guessed as shown in Figure 12. An erroneous guess for the methylene carbons has little practical consequence on the calculations because the tensor almost has axial symmetry.

**V.1.3. Definition of Sample Axes.** In all calculations the sample axis system was defined as having the z-axis perpendicular to the plane of the film. The y-axis was along the tenting direction and the x-axis was along the machine direction.

**V.2. Analysis of One- and Two-Dimensional Spectra.** The relatively sharp signals in the spectrum of

the film when its plane was perpendicular to the magnetic field (Figure 5a) suggest that there is a high degree of uniformity in the orientation of the molecules with respect to the film plane. Each of the narrow peaks for the perpendicular orientation is spread into a range of frequencies when the sample is rotated, however. This may be seen in the slices from the two-dimensional spectra as well as in the spectra of Figure 5b,c. There is a wide range of orientations of the polymer chains within the film plane.

It is helpful to know what kind of pattern would result if the polymer chains were distributed randomly in the film plane. Assume that the orientation of the molecular axis system of every polymer fragment with respect to the sample axis system can be described with the same Euler angles  $\alpha$  and  $\beta$ , but that there is uniform distribution of the angle  $\gamma$ . The key to determination of the overall NMR pattern resulting from all the molecules together is knowing how the chemical shift of a nucleus (a single fragment) is determined by the value of the angle  $\gamma$ .

The problem involved is equivalent to the calculation of the chemical shift of a nucleus in a molecule which is rotated with a goniometer about an axis perpendicular to the magnetic field. The nomenclature of Figure 2 can be used. The orientation of the PAS with respect to the molecular axis system is given by the Euler angles  $\alpha_1$ ,  $\beta_1$ , and  $\gamma_1$ . The molecule has an orientation with respect to the goniometer frame which is specified by the two sets of Euler angles  $\alpha$ ,  $\beta$ , and  $\gamma$  and  $\alpha'$ ,  $\beta'$ , and  $\gamma'$ . We assume that the  $z$ -axis of the goniometer frame coincides with the  $z$ -axis of the sample frame (which is perpendicular to the film plane). Thus  $\alpha''$  has an equivalent effect to  $\gamma$  in the original problem. The chemical shift tensor in the goniometer frame can be calculated from these angles through successive application of eq 2 (as shown in Mehring). The observed chemical shift is controlled by the set of angles  $\alpha''$ ,  $\beta''$ , and  $\gamma''$ , representing the orientation of the goniometer frame in the laboratory frame. The angle of rotation of the goniometer is specified by  $\alpha''$ . Overall we have

$$\omega = (1/2)(A_{11} + A_{22}) + (1/2)(A_{22} - A_{11}) \cos 2\alpha'' + (1/2)(A_{12} + A_{21}) \sin 2\alpha''$$

$$\omega = A + B \cos (2\alpha'' + \phi) \quad (4)$$

where  $\omega$  is the chemical shift,  $A_{ij}$  is an element of the chemical-shift tensor defined with respect to a coordinate system with the  $z$ -axis perpendicular to the plane,  $A = (1/2)(A_{11} + A_{22})$ ,  $B = (1/2)[(A_{22} - A_{11})^2 + (A_{12} + A_{21})^2]^{1/2}$ , and  $\phi = \tan^{-1} [(A_{22} - A_{11}) / (A_{12} + A_{21})]$ .

Opella and Waugh<sup>79</sup> and Spiess<sup>18</sup> have calculated the pattern given by an ensemble of molecules in a plane having arbitrary orientation with respect to the magnetic field when one of the axes of the PAS is perpendicular to the plane. The expression for the chemical shift has the same form as does eq 4. Thus the line-shape function  $S(\omega)$  in both cases is the same. Equation 5 describes a sym-

$$S(\omega) = (1/\pi)(B + A - \omega)^{-1/2}(B - A + \omega)^{-1/2} \quad (5)$$

metrical pattern with maximal intensity at the extreme values  $A + B$  and  $A - B$ .

The carbonyl spectra in Figures 7(1) and 9(1) come close to the ideal pattern although the edges of the pattern are unequal in intensity. The skewing suggests that the polymer chains are nonrandomly distributed within the film plane. The direction of the skewing should be reversed in Figures 7(1) and 9(1) if this interpretation is correct, but the underlying intensity from the aromatic carbons adds to the right-hand edge of the carbonyl pattern. The signal from the methylene carbons, to be dis-

cussed below, confirms that the polymer chains are preferentially aligned along the tenting direction in the film plane.

Table II can be used as a basis for calculation of the expected frequencies of maximum carbonyl intensity in Figures 5a, 7(1), and 9(1). Assume that the  $z$ - and  $x$ -axes used for the table lie in the film plane in the most probable orientation. This corresponds to the long axis of the polymer lying in the film plane and the plane of the aromatic ring lying almost parallel to the film plane. Calculation with eq 2 leads to a predicted shift of 112 ppm for the carbonyl carbon when the film plane is perpendicular to the magnetic field. The maximum carbonyl intensity in Figure 5a is 119 ppm. Equations 2 and 5 lead to predicted maxima of intensity in Figures 7(1) and 9(1) at 249 and 130 ppm, respectively, to be compared with the observed maxima at 247 and 129 ppm. All in all, the agreement between the predicted and observed values is close enough to indicate that the most favored orientation of the molecules relative to the film plane is close to that assumed.

VanderHart and co-workers observed the carbonyl signal at 245 ppm in highly oriented PET fibers aligned along the magnetic field.<sup>24</sup> The predicted chemical shift for the carbonyl based on Table II when the polymer is aligned along the magnetic field is 244 ppm. We conclude that the edge of the patterns of Figures 7(1) and 9(1) at 249 ppm corresponds to alignment of the polymer chains along the magnetic field. Because the intensity of that edge in Figure 9(1) is relatively greater than the intensity at the other edge (as compared with Figure 7(1)), in the most favored orientation in the PET films the polymer chain is along the tenting direction of the film.

The methylene carbons give rise to double-peaked patterns that are similar to those for the carbonyl carbons (Figures 7(1) and 9(1)). However, for the methylene carbons the intensities at the edges of the spectrum do reverse themselves, as expected, as the sample is rotated. The points of maximum intensity in the spectra of Figures 5a, 7(1), and 9(1) occur at 25, 80, and 77 ppm. Calculated values based on the structure of Table II are 25, 81, and 80. Again the agreement is good.

For VanderHart's fibers the methylene signal came at 24 ppm.<sup>24</sup> The predicted value is 27 ppm for alignment of the  $z$ -axis of Table II along the magnetic field. The most favored orientation of the polymer chains within the plane of the film in the tenting direction determined from the carbonyl signal is confirmed on the basis of the methylene signals in Figures 7(1) and 9(1).

There are three different types of aromatic carbons in PET. Overlap of the various signals from the three obscures some of the orientational information in the spectra although the relatively narrow signal at low frequency in Figure 5c does suggest that the rings are oriented almost parallel to the film plane. Calculations based on the molecular structure of Table II for the points of maximum intensity in the various spectra give 158, 215, and 19 ppm for carbon 5; 220, 151, and 21 ppm for carbon 4; and 222, 141, and 38 ppm for carbon 1. Agreement with the observed spectra is satisfactory.

In the oriented fibers the aromatic signals were reported to come at 157, 195, and 236 ppm<sup>24</sup> although the last value appears to be a misprint. The predicted values based on Table II are 159, 196, and 214 ppm.

The plane of the aromatic ring is tilted by about 10° with respect to the  $xz$  plane in the molecular axis system used for Table II. Calculations of the observed chemical shifts on the basis of axis systems rotated 10° either di-

**Table III**  
Measured Orientation Moments of  
Poly(ethylene terephthalate)

moment <sup>a</sup>	A <sup>b</sup>	B <sup>c</sup>	C <sup>c</sup>
$\hat{P}_{200}$	-0.31	0.48	0.50
$\hat{P}_{202}$	-0.13	-0.01	-0.02
$\hat{P}_{220}$	-0.26	0.06	0.14
$\hat{P}_{222}$	0.06	0.11	0.13
$\hat{P}_{400}$			0.36
$\hat{P}_{600}$			0.16

<sup>a</sup> Normalized so that  $\hat{P}_{000} = 1$ . Only those moments shown were allowed to vary in each simulation. <sup>b</sup> Calculated with the axis system used for Table II. <sup>c</sup> Calculated with an axis system rotated 90° about the *x*-axis from that used for Table II.

rection relative to that of Table II failed to improve the agreement with the observed values. In the crystal the rings are tilted with respect to the (100) plane. Thus the NMR results suggest that the rings are indeed tilted slightly from the plane of the film in the most favored orientation and the primary orienting entity in the ordered region is a microcrystal rather than the aromatic rings themselves. Previous X-ray results have shown that the (100) plane has a strong tendency to orient parallel to the plane of stretched PET.<sup>28</sup>

The broad background signal in Figure 5a results from a much less oriented fraction of the PET. Because this signal is suppressed in Figure 5b, it may be associated with that portion of the sample having a short proton spin-lattice relaxation time in the rotating frame. This is the less mobile part of the material which may be "amorphous", the quotes indicating the ambiguity of the designation. We conclude that the "amorphous" regions of Kodak Estar base are much less highly oriented with respect to a perpendicular to the plane of the film than are the "crystalline" regions.

**V.3. Orientation Moments Determined from the Three-Dimensional Spectrum.** As was explained above, the experimental three-dimensional NMR spectrum can be simulated as the weighted sum of calculated "subspectra". The weighting factors are the orientational moments. Initially the simulation was made with the molecular axis system used for Table II. The results are listed in column A of Table III. To save computer time, only every other point of the full three-dimensional spectrum was used in the analysis. Because signals of the amorphous and crystalline regions were not separated in the three-dimensional spectrum, the observed moments are an average for those of the amorphous and crystalline polymer.

If all the orientation moments are known for any value of *l* and a particular pair of sample and molecular axes, the moments for any other molecular or sample axes may, in principle, be found analytically. For rotation of the sample axes

$$\hat{P}'_{lm'n} = \sum_m \hat{P}_{lmn} D^l_{mm'}(\Omega) \quad (6)$$

where  $\Omega$  represents the Euler angles for rotation from the original molecular axis system to the new molecular axis system. For rotation of the molecular axes

$$\hat{P}'_{lmm'} = \sum_n \hat{P}_{lmn} D^l_{nn'}(\Omega) \quad (7)$$

where  $\Omega$  are the Euler angles for rotation from the new sample axis system to the original axis system. Note that the Euler angles describe rotation from the old to the new axes for change of the sample axes but rotation from the new to the old axes for change of the molecular axes.

The assumption of symmetry in either the sample or the molecule does place some restrictions on the interconversion from one axis system to another. If orthorhombic symmetry is to be preserved, the Euler angles must have values of 0°, 90°, or multiples thereof, for example. Thus it is not possible to calculate moments for a new molecular-axis system that is tilted only 10° from the moments of the old system.

We may, however, calculate moments for a molecular axis system that is rotated 90° about the *x*-axis from that used for Table II. The Euler angles for the rotation are  $\alpha = -90^\circ$ ,  $\beta = 90^\circ$ , and  $\gamma = 90^\circ$ . In the new molecular axis system the polymer long axis lies along the *y*-axis, and the *z*-axis is more or less perpendicular to the plane of the aromatic rings. The validity of the calculated moments was checked by direct simulation of the spectrum with a new set of calculated subspectra. The results are shown in column B of Table III.

In general, the simulations became unstable when subspectra corresponding to *l* > 2 were included in the analysis. For the new molecular-axis system described in the previous paragraph, inclusion of subspectra corresponding to the moments  $\hat{P}_{400}$  and  $\hat{P}_{600}$  in the simulations did give reasonable results. The moments found are shown in column C of Table III. The differences in the values in columns B and C are indicative of the truncation errors in the simulations.

The type of broadening used on the calculated subspectra affected the results only slightly. The range in the orientational moments with variations between Gaussian and Lorentzian broadening of various degrees was comparable to the difference between the values between columns B and C of Table III, or 1 and 4 of Table III.

The results are, of course, sensitive to some extent to the assumptions used in the analysis. For example, the exact orientation of the chemical-shift tensors with respect to the molecular axes is not known. The values of the principal elements of the chemical-shift tensor assumed are also subject to error, especially if polymer motion partially averages the chemical-shift tensors. Furthermore, the gauche as well as the trans conformation is present in the film, and the methylene signal, which is likely to be affected by a conformational change, is included in the analysis. No statistical analysis of the errors in the orientational moments was made because it is believed that the systematic errors outweigh the statistical errors.

The moments based on the molecular-axis systems of Table II (column A, Table III) again lead to the conclusion that the polymer chain has a strong tendency to lie in the plane of the film. The moment  $\hat{P}_{200}$  would have a value of -0.50 for perfect alignment in the plane. The observed value of -0.33 indicates a strong tendency for alignment of the chain in the plane of the film.

The moment  $\hat{P}_{220}$  is proportional to the average of  $\sin^2 \beta \cos(2\alpha)$ . Because  $\beta$  is close to 90° for most chains,  $\hat{P}_{220}$  effectively measures  $\cos(2\alpha)$  for these highly oriented molecules. The relatively large negative value of -0.26 observed shows that the plane of the aromatic rings tends to be oriented parallel to the plane of the film. Thus the moment analysis is consistent with the interpretation of the one- and two-dimensional spectra in terms of orientation of the aromatic ring toward the plane of the film.

The moment  $\hat{P}_{202}$  measures how the polymer chain is distributed in the plane of the film. The observed negative value shows that the chains have a stronger tendency to be aligned along the tenting than along the machine direction. Once again the results are in agreement with the previous analysis.

**Table IV**  
Matrix of Averages of Squared Direction Cosines<sup>a</sup>

molecular coordinate	sample coordinate		
	x	y	z
x	0.50	0.27	0.22
y	0.32	0.54	0.12
z	0.17	0.18	0.65

<sup>a</sup> For an axis system rotated 90° about the x-axis of that used for Table II.

The rotated molecular-axis system used for columns B and C of Table III is interesting because the z-axis is close to perpendicular to the aromatic ring (and the (100) plane of the crystal). The large positive value of  $\bar{P}_{200}$  in column B provides another indication of the orientation of the plane of the ring in the plane of the film.

Spies and co-workers have compiled a graph of the ratios of the moments  $\bar{P}_{100}$  in the situation that  $\sin \beta$  is Gaussian distributed.<sup>17</sup> For  $\bar{P}_{200} = 0.5$ ,  $\bar{P}_{400}$  should be about 0.16, and  $\bar{P}_{600}$  should be close to zero. Clearly this model is inappropriate for describing the orientation of the normal to the plane of the aromatic ring. A detailed analysis of other possible models was not made, however.

The moment  $\bar{P}_{200} = \langle (1/2)(3 \cos^2 \beta - 1) \rangle$ . From it  $\langle \cos^2 \beta \rangle$  may be found. Equations 4 and 5 permit determination of all the other mean-square direction cosines. The values found for the rotated molecular-axis system are tabulated in Table IV. The values from system C have been interchanged so that they correspond to the axis system used for system A in the table.

In the convention for Table IV the molecular y-axis lies along the polymer chain, and the molecular z-axis is close to the perpendicular to the aromatic rings. The sample z-axis is perpendicular to the plane of the film. The largest average direction cosine squared reflects the orientation of the molecular z-axis relative to the sample z-axis. The large magnitude reflects again the alignment of the aromatic rings in the plane of the film. The chain axis lies perpendicular to the normal of the film, but is slightly more aligned along the y-axis than along the x-axis. This confirms again the conclusions made on the basis of the one- and two-dimensional spectra.

**V.4. Alternative NMR Methods.** Recently, an alternative two-dimensional technique for analysis of molecular orientation in polymer samples spinning slowly at the magic angle has appeared.<sup>80</sup> Because the spinning concentrates the intensity of the spectrum into a few spinning sidebands, this method has a sensitivity advantage over those described above. In the general case, however, several different molecular orientations will map onto the spectral features in a two-dimensional experiment. Only with very highly oriented samples can a series of experiments be used to lift the degeneracy (see the discussion in the Theoretical Section). Thus, the spinning experiment will be most useful for samples in which either the sample or the film has axial symmetry.

## VI. Conclusions

Two- and three-dimensional <sup>13</sup>C NMR techniques are, in fact, useful means to expand the information that can be obtained about molecular orientation in PET films. The higher dimensional spectra help both to relieve the problem of overlap of the signals from chemically different carbons and to provide a basis for quantitative evaluation of the orientation distribution function. Experiments that take advantage of differences in proton relaxation times permit evaluation of differences in the orientation of the

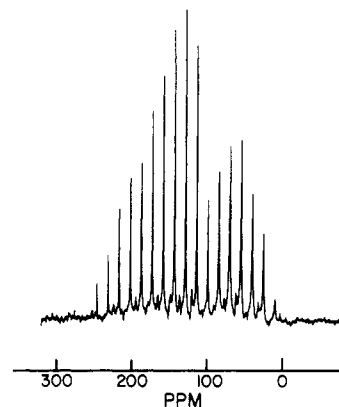


**Figure 13.** Spectrum obtained by Fourier transformation of a train of spin echoes obtained from a powder of poly(ethylene terephthalate). The "free-induction-decay" signal was weighted with a comb of exponential functions.

crystalline and amorphous regions of the sample.

**Acknowledgment.** I am indebted to R. W. Schrader for suggesting this project and to Dr. D. J. Massa for many useful discussions.

## VII. Appendix

Generation of three-dimensional NMR spectra is time consuming. Typically the spectra in this report required several days of data accumulation. Improvements in the inherent sensitivity of the NMR experiment could greatly shorten this time.

Recently Zilm has demonstrated that Fourier transformation of a spin-echo train generates a spectrum consisting of a series of spikes, the tops of which trace out the spectrum from Fourier transformation of the simple free-induction decay.<sup>81</sup> The overall signal-to-noise ratio in the spectrum is improved because the information in all of the echoes, rather than just the first decay, contributes to the spectrum. Such a spectrum from PET is shown in Figure 13.

The three-dimensional spectra for orientation measurements must necessarily be sampled coarsely. If the initial spectra in the generation of the full three-dimensional spectrum are generated by the echo technique, the points actually retained in the spectrum may be selected at the tops of the spikes resulting in an overall improvement in the signal-to-noise ratio.

The author has, in fact, created three-dimensional spectra in this manner, and they do have a lower noise level than do the standard spectra. Comparison of Figure 13 with Figure 4 shows that intensity in the methylene region is reduced in the echo spectrum, however. This probably results from a higher degree of mobility in the methylene region than in the rest of the molecule, which broadens the width of the individual spikes.<sup>82</sup> By itself this phenomenon is only a minor problem. The intensity of the methylene contribution to the spectra may be suppressed to compensate for the experimental reduction in intensity. A more serious problem is that the shape of the chemical-shift pattern will not be preserved when there is motional averaging. Typically the edges of the chemical-shift patterns are intensified relative to the centers.

The width of the individual spikes in the echo spectrum is determined by the rate at which the echo-train decays and thus is a  $T_2$  effect. Distortions introduced by variations of  $T_2$  among the various carbons and across the spectral patterns are relatively large because the total sampling times are large compared to the values of  $T_2$ . By

contrast, the distortions caused by variations in  $T_1$  in the rotation experiment are very small, because the rotation time is very small compared to  $T_1$ .

In practice the degree of orientation measured from the echo spectrum (as reflected by the apparent orientation moments) was larger than that determined from the standard spectrum, suggesting that indeed the spectral patterns were distorted in an undesirable way. The echo method may be useful in other systems in which motional averaging does not occur.

Registry No. PET, 25038-59-9.

## References and Notes

- Ward, I. M., Ed. *Structure and Properties of Oriented Polymers*; Wiley: New York, 1975.
- Chu, W. H.; Smith, T. L. In *Polymer Science and Technology*; Lenz, R. W., Stein, R. S., Eds.; Plenum: New York, 1973; Vol. 1, p 67.
- Schuur, G.; Van der Vegt, A. K. In ref 1, p 413.
- Arnoldsussen, T. C.; Rossi, E. M. *Annu. Rev. Mater. Sci.* **1985**, *15*, 379.
- Hughes, M. A.; Sheldon, R. P. *J. Appl. Polym. Sci.* **1964**, *8*, 1541.
- Bonart, R. *Kolloid Z. Z. Polym.* **1966**, *213*, 1.
- Morel, J. F.; Dung, P. N.; Joly, J. C. *IEEE Trans. Electr. Insul.* **1980**, *EI-15*, 335.
- Desai, P.; Abhiraman, A. S. *J. Poly. Sci., Polym. Phys. Ed.* **1985**, *28*, 653.
- Heffelfinger, C. J.; Lippert, E. L., Jr. *J. Appl. Poly. Sci.* **1971**, *15*, 2699.
- Biangardi, H. J.; Zachmann, H. G. *J. Polym. Sci., Polym. Symp.* **1977**, *58*, 169.
- Biangardi, H. J.; Zachmann, H. G. *Makromol. Chem.* **1976**, *177*, 1173.
- Slonim, I. Ya.; Urman, Ya. G. *Zh. Strukt. Khim., Eng. Ed.* **1963**, *4*, 192.
- McBrierty, V. J.; Douglass, D. C. *Macromol. Rev.* **1981**, *16*, 295.
- Folkes, M. J.; Ward, I. M. In ref 1, p 219.
- Farrow, G.; Ward, I. M. *Br. J. Appl. Phys.* **1960**, *11*, 543.
- Ito, M.; Kanamoto, T.; Tanaka, K.; Porter, R. S. *J. Polym. Sci., Polym. Phys. Ed.* **1985**, *23*, 59.
- Hentschel, R.; Sillescu, H.; Spiess, H. W. *Polymer* **1981**, *22*, 1516.
- Spiess, H. W. In *Developments in Oriented Polymers*, Ward, I. M., Ed.; Applied Science Publishers: London, 1982; p 47.
- Brandolini, A. J.; Apple, T. M.; Dybowski, C.; Pemberton, R. G. *Polymer* **1982**, *23*, 39.
- Brandolini, A. J.; Dybowski, C. *J. Polym. Sci., Polym. Lett. Ed.* **1983**, *21*, 423.
- Brandolini, A. J.; Alvey, M. D.; Dybowski, C. *J. Polym. Sci., Polym. Phys. Ed.* **1983**, *21*, 2511.
- Brandolini, A. J.; Rocco, K. J.; Dybowski, C. R. *Macromolecules* **1984**, *17*, 1455.
- Horii, F.; Kitamaru, R.; Maeda, S.; Terao, T. *Polym. Bull.* **1985**, *13*, 179.
- VanderHart, D. L.; Bohm, G. G. A.; Mochel, V. D. *Polym. Prepr. (Am. Chem. Soc., Div. Polym. Chem.)* **1981**, *22*, 261.
- VanderHart, D. L. *Macromolecules* **1979**, *12*, 1232.
- Hempel, G. *Plaste Kautsch.* **1981**, *28*, 378.
- Hempel, G.; Schneider, H. *Pure Appl. Chem.* **1982**, *54*, 635.
- Dulmage, W. J.; Geddes, A. L. *J. Polym. Sci.* **1958**, *31*, 499.
- Heffelfinger, C. J.; Burton, R. L. *J. Polym. Sci.* **1960**, *47*, 289.
- Heffelfinger, C. J.; Schmidt, P. G. *J. Appl. Sci.* **1965**, *9*, 2661.
- Zachmann, H. G. *Polym. Eng. Sci.* **1979**, *19*, 966.
- Boye, C. A.; Goodlett, V. W. *J. Appl. Phys.* **1963**, *34*, 59.
- Blumentritt, B. F. *J. Appl. Polym. Sci.* **1979**, *23*, 3205.
- Pereira, J. R. C.; Porter, R. S. *J. Polym. Sci., Polym. Phys. Ed.* **1983**, *21*, 1133, 1147.
- Kashiwagi, M.; Cunningham, A.; Manuel, A. J.; Ward, I. M. *Polymer* **1973**, *14*, 111.
- DeVries, A. J.; Bonnebat, C.; Beutemps, J. J. *J. Polym. Sci., Polym. Symp.* **1977**, *58*, 109.
- Jungnickel, B.-J. *Angew. Makromol. Chem.* **1980**, *91*, 203.
- Jungnickel, B.-J. *Prog. Colloid Polym. Sci.* **1980**, *67*, 159.
- Itoyama, K. *Kobunshi Ronbunshu (Engl. Ed.)* **1976**, *5*, 592.
- More generally this axis system is fixed in the smallest orienting structural unit, which could be a crystallite rather than the molecule itself.
- Hentschel, R.; Schlitter, J.; Spiess, H. W. *J. Chem. Phys.* **1978**, *68*, 56.
- White, J. L.; Spruiell, J. E. *Polym. Eng. Sci.* **1981**, *21*, 859.
- Bower, D. I. *J. Polym. Sci., Polym. Phys. Ed.* **1981**, *19*, 93.
- McBrierty, V. J. *J. Chem. Phys.* **1972**, *57*, 3287.
- McBrierty, V. J. *J. Chem. Phys.* **1974**, *61*, 872.
- Roe, R.-J.; Krigbaum, W. R. *J. Chem. Phys.* **1964**, *40*, 2608.
- Roe, R.-J. *J. Polym. Sci., Polym. Phys. Ed.* **1970**, *8*, 1187.
- Roe, R.-J. *J. Appl. Phys.* **1964**, *36*, 2024.
- Brink, D. M.; Satchler, G. R. *Angular Momentum*; Oxford: New York, 1962.
- The magnitudes of the orientation moments differ from author to author because of differences in the definitions of the expansion functions and in the normalization procedures. The appropriate correction factors required for comparison of results may be determined by comparison of the basis functions.
- From a practical point of view some symmetry in either the molecule or the sample is necessary for the moment description to be useful. Consider, for example, the problems of describing molecular orientation in a racemic mixture of optically active molecules. A right-handed reference axis system may, of course, be defined with respect to one of the molecular isomers. Another right-handed system may be placed in the sample. A right-handed axis system cannot be placed in the other second molecular isomer in a manner analogous to the way it was placed in the first, however. For any placement of the axis system actually chosen, the orientational distribution function for the second isomer will be different from that for the first when the sample itself has a nonsuperimposable mirror image. In practice, planes of symmetry in both the samples and the molecule have always been assumed in orientation problems.
- The convention of Hentschel, Schlitter, and Spiess defines the molecular orientation in terms of rotation from the molecule to the sample.<sup>41</sup> Care must be taken in comparison of results obtained with this convention with those found with the convention of Jarvis, Hutchinson, Bower, and Ward<sup>53</sup> and others, who treat the orientation in terms of rotations from the sample to the molecule. The roles of  $m$  and  $n$  are reversed in the two systems.
- Jarvis, D. A.; Hutchinson, I. J.; Bower, D. I.; Ward, I. M. *Polymer* **1980**, *21*, 41.
- McBrierty, V. J.; McDonald, I. R.; Ward, I. M. *J. Phys. D* **1977**, *4*, 88.
- Mehring, M. *High Resolution NMR Spectroscopy in Solids*; Springer Verlag: New York, 1976.
- Haebleren, U. *High Resolution NMR in Solids*, Academic: New York, 1976.
- Maciel, G. E.; Szeverenyi, N. M.; Sardashti, M. J. *Magn. Reson.* **1985**, *64*, 365.
- Bax, A.; Szeverenyi, N. M.; Maciel, G. E. *J. Magn. Reson.* **1983**, *52*, 147.
- Bax, A.; Szeverenyi, N. M.; Maciel, G. E. *J. Magn. Reson.* **1983**, *55*, 494.
- Carter, C. M.; Alderman, D. W.; Grant, D. M. *J. Magn. Reson.* **1985**, *65*, 183.
- Spiess, H. W. *NMR: Basic Princ. Prog.* **1978**, *15*, 55.
- Henrichs, P. M.; Young, R. H.; Hewitt, J. M. *J. Magn. Reson.* **1986**, *69*, 460.
- Murphy, P. D.; Taki, T.; Gerstein, B. C.; Henrichs, P. M.; Massa, D. J. *J. Magn. Reson.* **1982**, *49*, 99.
- English, A. D. *Macromolecules* **1984**, *17*, 2182.
- Schmidt, P. G. *J. Polym. Sci., Part A* **1963**, *1*, 1271.
- Hsu, B.-S.; Kwan, S.-H.; Wong, L.-W. *J. Polym. Sci., Polym. Phys. Ed.* **1975**, *13*, 2079.
- Cunningham, A.; Ward, I. M.; Willis, H. A.; Zichy, B. *Polymer* **1974**, *15*, 749.
- Fina, L. J.; Koenig, J. L. *Macromolecules* **1984**, *17*, 2572.
- Koenig, J. L.; Hannon, M. J. *J. Macromol. Sci., Phys.* **1967**, *B1*, 119.
- Ito, M.; Pereira, J. R. C.; Hsu, S. L.; Porter, R. S. *J. Polym. Sci., Polym. Phys. Ed.* **1983**, *21*, 389.
- VanderHart, D. L.; Khoury, F. *Polymer* **1984**, *25*, 1589.
- Gibby, M.; Pines, A.; Waugh, J. S. *Chem. Phys. Lett.* **1972**, *16*, 296.
- Tegenfeldt, J.; Sjöblom, R. *J. Magn. Reson.* **1983**, *55*, 372.
- Havens, J. R.; VanderHart, D. L. *Macromolecules* **1985**, *18*, 1663.
- VanderHart, D. L., personal communication.
- Such rotation is possible if the turning axis is aligned at the magic angle with respect to the magnetic field. In the initial orientation one of the symmetry axes of the sample should lie parallel to the magnetic field. The rotation axis should lie parallel to the film plane. The author is grateful to Dr. David VanderHart for pointing out this possibility.

- (77) Daubeny, R. de P.; Bunn, C. W.; Brown, C. J. *Proc. R. Soc. (A)* **1954**, *14*, 531.  
 (78) Cunningham, A.; Manuel, A. J.; Ward, I. M. *Polymer* **1976**, *17*, 125.  
 (79) Opella, S. J.; Waugh, J. S. *J. Chem. Phys.* **1977**, *66*, 4919.  
 (80) Harbison, G. S.; Spiess, H. W. *Chem. Phys. Lett.* **1986**, *124*, 128.  
 (81) Zilm, K. W., personal communication.  
 (82) Swanson, S.; Ganapathy, S.; Kennedy, S.; Henrichs, P. M.; Bryant, R. G. *J. Magn. Reson.* **1986**, *69*, 531.

## Analysis of Surface Structures in Nitrogen-Containing Polymer Systems by Ion Scattering Spectroscopy

Kevin J. Hook and Joseph A. Gardella, Jr.\*

Department of Chemistry, State University of New York at Buffalo,  
Buffalo, New York 14214

Lawrence Salvati, Jr.

Perkin Elmer Physical Electronics Laboratories, Edison, New Jersey 08820.

Received February 2, 1987

**ABSTRACT:** Low-energy ion scattering spectroscopy (LEIS or ISS) combined with molecular mechanics calculations is used to predict the structure and orientation of functional groups at the topmost surface for a group of nitrogen-containing polymers. ISS of poly(2-vinylpyridine) (P2VP), poly(4-vinylpyridine) (P4VP), and ethylated P2VP gives N/C scattered ion intensity ratios which reflect the position of the nitrogen in the planar side group. The N/C scattered intensity ratios were  $0.404 \pm 0.025$  for P4VP,  $0.01 \pm 0.02$  for P2VP, and  $0.42 \pm 0.025$  for ethylated P2VP. Results are explained through the use of conformational energy calculations, classical concepts such as "shadowing" and "shielding" effects, and molecular modeling. X-ray photoelectron spectroscopy (XPS or ESCA) data show no differences between P2VP (ortho nitrogen) and P4VP (para nitrogen). ISS of poly(vinylpyrrolidone) (PVPyr) and poly(vinylcarbazole) (PVK) is used to complement the work done on the pyridine polymers. The combined data support a polymer orientation in which the polymer backbone is exposed to the vacuum at the vacuum/surface interface. These results are possible because of the extreme surface sensitivity of the ISS technique.

### Introduction

ISS is a surface analytical technique which samples a shallow surface region (3–5 Å) and thus gives direct and indirect information on surface composition, structure, molecular orientation, and morphology.<sup>1,2</sup> The principle behind ISS is quite straightforward. Typically, a monoenergetic beam of noble gas ions such as <sup>3</sup>He, <sup>4</sup>He, or <sup>20</sup>Ne is scattered from a surface with the energy of the scattered ion dependent upon the atomic composition of the surface. The energetics of the scattering event can be described by using the following equation which is derived from the laws of conservation of energy and momentum:<sup>1</sup>

$$\frac{E_1}{E_0} = \frac{M_1^2}{(M_1 + M_2)^2} \left[ \cos \theta + \left( \frac{M_2^2}{M_1^2} - \sin^2 \theta \right)^{1/2} \right]^2 \quad (1)$$

where  $E_0$  and  $E_1$  represent the energy of the ions before and after the scattering event,  $M_1$  and  $M_2$  represent the masses of the primary ion and of the surface atom, respectively, and  $\theta$  is the laboratory scattering angle.

As Niehus and Comsa point out, sensitivity to the first atomic layer is due to the severe neutralization of the noble gas ions used in the ISS technique.<sup>3</sup> Practically none of the incident ions that penetrate farther into the sample than the first layer are able to scatter into the vacuum as an ion. The high neutralization probability of the ion is the result of the occupation of an atomic state by a surface electron that occurs because of coupling to the solid. A noble gas ion incident with a surface presents a deep potential well for an electron (–24.6 eV for He, –21.6 eV for Ne, and –15.8 eV for Ar) compared with the work function of a solid (about 2–5 eV),<sup>4,5</sup> the result being that during a scattering event the surface electron can neutralize the

incident ion. Charge capture largely occurs via both one-electron resonant and two-electron Auger processes, with the dominant process being highly dependent on the specific energetics of the ion–surface interaction.<sup>5–8</sup>

The interaction between the incident ion and a surface atom results in the formation of areas which are effectively shielded from the possibility of undergoing a collision with the incoming ion beam. The interaction can be described classically through the use of a "shadow" cone.<sup>9</sup> Because of the low-energy conditions used in this technique, incoming ions are scattered by a relatively weak potential which is effectively described by the screened Coulomb potential.<sup>1,9</sup> As discussed in our previous paper,<sup>2</sup> "shielding" and "shadowing" represent two different conditions. The term shadowing means the situation when an atom heavier than <sup>3</sup>He prevents ion scattering from atoms lying underneath. The term shielding in this case will describe the situation when an atom lighter than the primary ion slightly deflects or is sputtered by the primary ion. The slight deflection does not utilize hydrogen as the scattering center. However, as observed by Diehl,<sup>10</sup> this prevents ion scattering from occurring and affects relative intensities.

It is important in ISS to address certain limitations which are inherent in the technique. Of primary concern is the difficulty in resolving spectral peaks which are broad and suffer from large overlap. Secondly, as can be seen in eq 1, the ISS method cannot detect elements lighter than <sup>3</sup>He. However, weakly adsorbed hydrogen does produce inelastic scattering effects which are evident in the overall appearance of the spectrum, the result being a large background which further complicates spectral interpretation. Another limitation, the inability to obtain absolute primary ion intensities, will force reliance on relative ion intensity ratios to obtain quantitative information. Nevertheless, because of the extreme surface

\* Author to whom correspondence should be addressed.